

Journal Electronic Materials

Revised

July 4, 2014

Zinc Oxide Thin-Film Transistors Fabricated at Low Temperature by Chemical Spray Pyrolysis

Yesul Jeong¹, Christopher Pearson¹, Yong Uk Lee², Lee Winchester², Jaeun Hwang³, Hongdoo Kim³, Lee-Mi Do⁴ and Michael C Petty^{1,*}

¹*School of Engineering and Computing Sciences and Centre for Molecular and Nanoscale Electronics, Durham University, South Road, Durham DH1 3LE, UK.*

²*Centre for Process Innovation Limited, Thomas Wright Way, Sedgfield, Durham TS21 3FG, UK.*

³*Department of Advanced Materials Engineering for Information and Electronics, Kyung Hee University, Yongin 446-701, Korea.*

⁴*IT Convergence Technology Research Laboratory, Electronics and Telecommunications Research Institute, Daejeon, Korea.*

E-mail: m.c.petty@durham.ac.uk

We report on the electrical behaviour of undoped zinc oxide thin film transistors (TFTs) fabricated using low temperature chemical spray pyrolysis. An aerosol system utilizing aerodynamic focusing was used to deposit the ZnO. Polycrystalline films were subsequently formed by annealing at the relatively low temperature of 140 °C. The TFTs possessed a saturation mobility of 2 cm²/Vs, which is the highest reported for undoped ZnO TFTs manufactured below 150 °C. The devices also exhibited an on/off ratio of 10⁴ and a threshold voltage of -3.5 V. These parameters were found to depend reversibly on the measurement ambient.

Keywords: zinc oxide transistors; chemical spray pyrolysis; environmental effects

INTRODUCTION

Zinc oxide semiconductors are currently the subject of considerable academic and commercial interest. These compounds could form the basis of thin film transistor (TFT) technologies for applications in flexible, large-area electronics. The attraction of such materials derives from their relatively high charge carrier mobilities and optical transparency. Much of the research is being undertaken with doped ZnO semiconductors, such as indium-doped ZnO (IZO)¹⁻³ or indium-gallium-doped ZnO (IGZO).³ However, devices using undoped ZnO are preferable due to the limited availability and high cost of indium. Solution processing offers the additional advantages of simple and low-cost device fabrication. There has been encouraging progress with ZnO. Using spin-coating, Yu et al.⁴ achieved a mobility of 4 cm²/Vs for devices fabricated at 300 °C, while Xu et al.⁵ and Jun et al.⁶ have demonstrated mobilities of approximately 0.5 cm²/Vs using the same processing method, but with a 150 °C annealing temperature.

Chemical spray pyrolysis,^{7,8} ink-jet printing^{1,9} and spin coating^{3,10} are widely believed to be promising methods for realizing low-cost manufacture and large-scale processing. Chemical spray pyrolysis involves the vaporization of a precursor solution and subsequent transport of the resulting mist to a heated substrate where it reacts to form a thin film of the desired material. Here, we report on the use of spray coating using an aerosol jet to fabricate undoped ZnO TFTs at the relatively low process temperature of 140 °C. The jet printing method exploits aerodynamic focusing to deposit the precursor material with precision onto a substrate. The technique offers direct patterning of material so that wastage is minimized and the processing speed is increased. The influence of the measurement environment on the performance of the aerosol-printed TFTs is also investigated.

EXPERIMENTAL PROCEDURES

A schematic diagram of the bottom-gate, top-contact TFT structure used in this work is shown in Fig. 1(a). An n⁺ Si substrate served as the gate electrode while an 85 nm thick layer of SiO₂, grown by

thermal oxidation, was used as the gate insulator. Before coating, the SiO₂ was treated with an UV ozone plasma, which resulted in a hydrophilic surface. The precursor solution was formed by dissolving 0.081 g of zinc oxide (Sigma-Aldrich, ≥99.9%) in 9.8 g of ammonium hydroxide (NH₄OH). This was then placed into a refrigerator for one day, leading to a fully transparent fluid. The semiconductor solution was deposited by the aerosol jet printing method (M3D 300CE system, Optomec Inc.). An ultrasonication unit (applied voltage 42 V) was used to vaporize the oxide ink solution. The flow rates of the atomizer gas used for carrying the mist and the sheath gas for controlling the size of the patterns were 28 cm³/min and 40 cm³/min, respectively. A 300 μm diameter ceramic deposition tip was used and the printing stage speed was 2 mm/s. The substrates were moved to the hotplate for drying within 3 seconds after the printing. Following deposition, the thin films were annealed in air for 30 min at 140 °C. Aluminium source (S) and drain (D) electrodes (50 nm in thickness) were defined by thermal evaporation through a shadow mask, under a vacuum of approximately 2x10⁻⁶ mbar; the channel length and width were 200 μm and 4000 μm, respectively. The surface morphologies of the thin films were studied using a Digital Instruments Nanoman II Atomic Force Microscope (AFM). Electrical characterization of the transistors was undertaken in the dark, in either air or vacuum (~10⁻² mbar) ambients, using a Keithley 485 picoammeter. Experiments in different humidity environments were undertaken using a ESPEC CORP. SH-641 Bench-top Type Temperature & Humidity Chamber. Figure 1(b) reveals a typical 5 μm x 5 μm AFM image of the surface of a spray-coated ZnO thin film on a Si/SiO₂ substrate; the average thickness of the deposited oxide material, measured by a Dektak profilometer, was 183 nm. Grains of ZnO are evenly distributed across the surface; the arithmetic average roughness and grain size for this ZnO thin film, obtained from the AFM image, are approximately 30 nm and 100 nm, respectively. The surface morphology is quite similar to that reported by Jun et al.⁶ for ZnO fabricated by spin coating, suggesting that the thin film could be suitable for the active layer in TFTs.

RESULTS AND DISCUSSION

Figure 2(a) shows the drain-to-source current versus the drain-to-source voltage (I_{DS} - V_{DS}) characteristics of a ZnO TFT measured in an air environment; the gate voltage (V_G) was varied from 0 V to

50 V, in 10 V increments. The output characteristics of this device show typical n-channel operation. The curves reveal reasonable linear and saturation regions with little hysteresis between the forward and reverse V_{DS} scans. In addition, a clear pinch-off and a high saturation current, of about 2×10^{-3} A for $V_{DS} = 60$ V and $V_G = 50$ V, are achieved.

The transfer characteristic for the device measured in an air environment is shown in Fig. 2(b). The drain-to-source voltage was fixed at 80 V, while V_G was swept reversibly from -10 V to 50 V. On application of a positive gate bias, I_{DS} increases sharply, with a small degree of hysteresis observed when the scan direction was reversed. The threshold voltage (V_{TH}), sub-threshold slope and on/off ratio, extracted from this transfer characteristic, are -3.5 V, 0.5 V/decade and $\sim 10^4$. The saturation field effect mobility, which was derived from the slope of the graph of $I_{DS}^{1/2}$ versus V_G , is $2.0 \text{ cm}^2/\text{Vs}$.

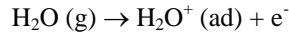
These results should be contrasted to other reports on ZnO TFTs produced by spray pyrolysis. For example, Bashir et al.⁷⁾ examined transistors and circuits processed at temperatures of 200 °C to 500 °C. The carrier mobility for devices fabricated at 200 °C was $0.13 \text{ cm}^2/\text{Vs}$; in contrast, for TFTs processed at 400 °C, the mobility was $15 \text{ cm}^2/\text{Vs}$, the highest value achieved in this study. Similar work by Adamopoulos et al.,¹¹ for devices processed at 400 °C and using optimized S/D electrodes, exhibited a mobility of 10 to $22 \text{ cm}^2/\text{Vs}$. These workers also reported that the formation of polycrystalline ZnO could be achieved at temperatures above 200 °C and that, under these conditions, the mobility was around $0.003 \text{ cm}^2/\text{Vs}$, while a maximum mobility of $25 \text{ cm}^2/\text{Vs}$ could be obtained at temperatures above 400 °C.¹² More recently, a study by Faber et al.⁸ showed similar results for ZnO TFTs (carrier mobility $\sim 0.18 \text{ cm}^2/\text{Vs}$) fabricated entirely by the spray pyrolysis of different precursor compounds. This report suggests a potential route to a fully solution-based device. Although the carrier mobility in our TFTs is somewhat lower than other reports, it is notable that a relatively low device processing temperature, 140 °C, is used. To our knowledge, the figure of $2 \text{ cm}^2/\text{Vs}$ for the carrier mobility in our devices is the highest reported to date for undoped ZnO TFTs manufactured below 150 °C. At present, we can offer no detailed explanation for this relatively high mobility achieved at low temperatures. The transistor configuration that we have used is standard. The most likely explanation therefore lies in the processing of the zinc oxide solution and its deposition. Many groups use a zinc acetate ($\text{Zn}(\text{CH}_3\text{CO}_2)_2$) precursor solution, which requires a relatively high annealing temperature for conversion to ZnO. Annealing at sub-optimum temperatures may leave a residue of carbon atoms, which can act as carrier

trapping sites. In this study, we use zinc oxide directly dissolved in ammonium hydroxide. This offers a simpler approach for producing carbon-free ZnO films. Clearly, further work is needed to clarify this.

It is now established that the sensitivity to absorbed molecules is an important factor in determining the stability of ZnO-based TFTs.¹³ An initial investigation on the effects of the measuring environment on the electrical properties of our TFTs was therefore undertaken. These results are presented in Fig. 3. The transfer curve was first obtained in an air environment, with V_{DS} held at 80 V while V_G was swept from -10 to 50 V, in 10 V increments. Next, the device was kept under a vacuum of approximately 10^{-2} mbar for two days before the measurements were taken. A final experiment was performed two days after breaking the vacuum. Under vacuum, the drain current decreased from 1.1×10^{-3} A to 4.5×10^{-5} A at $V_G = 50$ V. Following re-exposure to air, I_{DS} increased rapidly to its original value. The various parameters including saturation field effect mobility, V_{TH} , and on/off ratio under the different environmental conditions are summarized in Table 1. The saturation field effect mobility decreased from $2 \text{ cm}^2/\text{Vs}$ in air to $0.5 \text{ cm}^2/\text{Vs}$ under vacuum and then increased to $1.8 \text{ cm}^2/\text{Vs}$ after re-exposure to air, almost achieving the original air value. In contrast, the device on/off ratio increased about one order of magnitude in vacuum, to $\sim 10^5$, resulting from the decrease in the device off-current.

Oxygen from an air environment is usually the dominant factor in the degradation of the performance of ZnO TFTs.^{13,14} This is because absorbed O_2 molecules capture carriers in the ZnO thin film, which produces an upward bending of the conduction band. The creation of a depletion layer near the surface also decreases the mobility of the remaining carriers. It is believed that a vacuum environment leads to improved electrical performance because of the desorption of such contamination molecules.¹⁵ Our study appears to show the opposite effect, i.e. that the carrier mobility is enhanced in an air environment. However, an alternative explanation becomes apparent on noting that the air ambient will contain both oxygen and water molecules. The competing effects of these molecular species on the UV photoresponse of ZnO nanowires has been noted previously.¹⁴

We suggest that the ZnO thin films produced in our work incorporate a relatively large number of OH groups, compared with ZnO films fabricated at higher temperatures. Under an air environment, the dominant effect may be the attraction of water molecules rather than oxygen molecules to the semiconductor surface, decreasing the depletion region or even producing a region of electron accumulation, i.e.



This would account for the increase in mobility and negative shift of V_{TH} .¹⁶ In addition, this accumulation layer might cause an increase in the device off-current in the low V_{GS} region, resulting in the formation of a high conduction path between source and drain. Under vacuum, the water molecules are removed, leading to an increased depletion region, and a lower carrier concentration. These H_2O effects on ZnO thin films are in agreement with the research reported by other groups.^{13,16,17} To test this hypothesis, we have measured our TFT characteristics in an environmental chamber at room temperature, but under different humidities (RH). The results are shown in Figure 4. Above a RH of 50%, both the carrier mobility and threshold voltage are relatively constant. However, as the RH is reduced to 35% (the minimum value attainable in our environmental chamber) the carrier mobility falls while V_{TH} shifts towards more positive voltages. This preliminary experiment supports our idea outlined above.

CONCLUSIONS

In summary, we report the use of aerosol jet printing for the fabrication of undoped ZnO TFTs. A carrier mobility of approximately $2 \text{ cm}^2/\text{Vs}$ is achieved with a relatively low processing temperature of $140 \text{ }^\circ\text{C}$. A preliminary study reveals that the TFT performance is influenced by the measurement ambient. A full understanding of these phenomena is clearly needed. However, we suggest that our results augur well for the low-temperature solution processing of undoped ZnO transistors.

Acknowledgements

This work was supported by the Industrial Strategic Technology Development Program (10041808, Synthesis of Oxide Semiconductor and Insulator Ink Materials and Process Development for Printed

Backplane of Flexible Displays Processed Below 150°C) funded by the Ministry of Knowledge Economy (MKE, Korea)

REFERENCES

1. S. Lee, J. Kim, J. Choi, H. Park, J. Ha, Y. Kim, J. A. Rogers, and U. Paik, *Appl. Phys. Lett.* **100** (10), 102108 (2012).
2. J. H. Park, S. J. Lee, T. I. Lee, J. H. Kim, C. -H. Kim, G. S. Chae, M. -H. Ham, H. K. Baik, and J. -M. Myoung, *J. Mater. Chem.* **C 1** (9), 1840 (2013).
3. Y. S. Rim, W. H. Dong, J. L. Kim, H. S. Lim, K. M. Kim, and H. J. Kim, *J. Mater. Chem.* **22**, 12491 (2012).
4. S. H. Yu, B. J. Kim, M. S. Kang, S. H. Kim, J. H. Han, J. Y. Lee, and J. H. Cho, *ACS Appl. Mater. Interfaces* **5** (19), 9765 (2013).
5. X. Xu, Q. Cui, Y. Jin, and X. Guo, *Appl. Phys. Lett.* **101** (22), 222114 (2012).
6. T. Jun, K. Song, Y. Jeong, K. Woo, D. Kim, C. Bae, and J. Moon, *J. Mater. Chem.* **21** (4), 1102 (2011).
7. A. Bashir, P. H. Wöbkenberg, J. Smith, J. M. Ball, G. Adamopoulos, D. D. C. Bradley, and T. D. Anthopoulos, *Adv. Mater.* **21** (21), 2226 (2009).
8. H. Faber, B. Butz, C. Dieker, E. Spiecker, and M. Halik, *Adv. Funct. Mater.* **23**, 2828 (2013).
9. Y. -J. Kwack and W. -S. Choi, *IEEE Electron Device Lett.* **34**, 78 (2013).
10. K. -B. Park, J. -B. Seon, G. H. Kim, M. Yang, B. Koo, H. J. Kim, M. -K. Ryu, and S. -Y. Lee, *IEEE Electron Device Lett.* **31** (4), 311 (2010).
11. G. Adamopoulos, A. Bashir, P. H. Wöbkenberg, D. D. C. Bradley, and T. D. Anthopoulos, *Appl. Phys. Lett.* **95** (13), 133507 (2009).
12. G. Adamopoulos, A. Bashir, W. P. Gillin, S. Georgakopoulos, M. Shkunov, M. A. Baklar, N. Stingelin, D. D. C. Bradley, and T. D. Anthopoulos, *Adv. Funct. Mater.* **21** (3), 525 (2011).
13. J. K. Jeong, H. W. Yang, J. H. Jeong, Y. -G. Mo, and H. D. Kim, *Appl. Phys. Lett.* **93** (12), 123508 (2008).
14. Y. Li, F. D. Valle, M. Simonnet, I. Yamada, and J. -J. Delaunay, *Appl. Phys. Lett.* **94** (2), 023110 (2009).
15. S. Song, W. -K. Hong, S. -S. Kwon, and T. Lee, *Appl. Phys. Lett.* **92** (26), 263109 (2008).

16. W. -F. Chung, T. -C. Chang, H. -W. Li, C. -W. Chen, Y. -C. Chen, S. - C. Chen, T. -Y. Tseng, and Y. -H. Tai, *Electrochemical and Solid State Lett.* 14 (3) H114-H116 (2011).
17. J.-S. Park, J. K. Jeong, H. -J. Chung, Y. -G. Mo, and H. D. Kim, *Appl. Phys. Lett.* 92 (7), 072104 (2008).

Figure and Table Captions

Fig. 1. (a) Schematic diagram of the bottom-gate, top-contact ZnO TFT structure. (b) AFM topography image of a ZnO thin film on a Si/SiO₂ substrate deposited using aerosol jet printing, followed by annealing at 140 °C.

Fig. 2. (a) Output characteristics of a top contact ZnO TFT ($L = 200 \mu\text{m}$, $W = 4000 \mu\text{m}$), (b) Transfer characteristics in the saturation region ($V_{DS} = 80 \text{ V}$).

Fig. 3. (a) Transfer characteristics in the saturation region ($V_{DS} = 80 \text{ V}$), measured in air (-■-: forward sweep, -□-: reverse sweep), under vacuum for two days (-●-: forward sweep, -○-: reverse sweep), and again in air for two days (-▲-: forward sweep, -△-: reverse sweep) .

Fig. 5. Carrier mobility and threshold voltage for ZnO TFTs measured at room temperature under different humidity ambients.

Table 1. Summary of the electrical characteristics for a ZnO TFTs as a function of the measurement environment.

	Mobility (cm ² /Vs)	On/off ratio	V _{TH} (V)
Air	2.0	~10 ⁴	-5.4
Vacuum	0.5	~10 ⁵	-3.5
Air	1.8	~10 ⁴	-7.1

Table 1

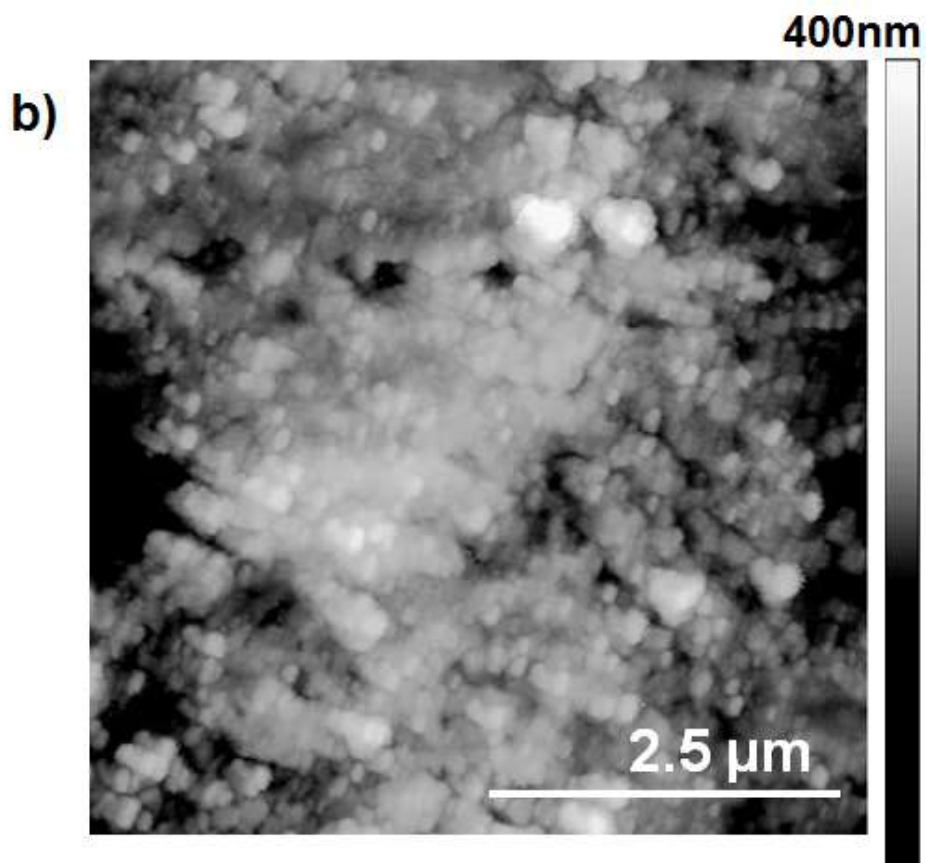
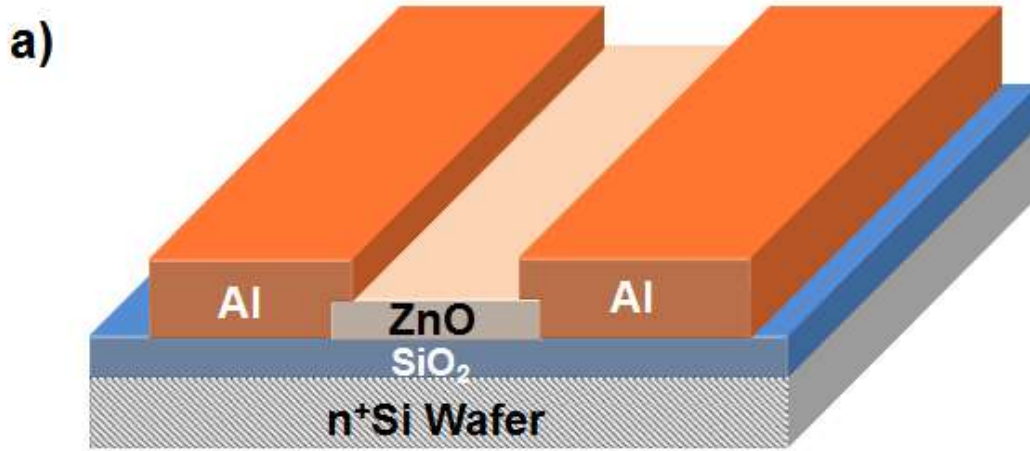


Fig 1

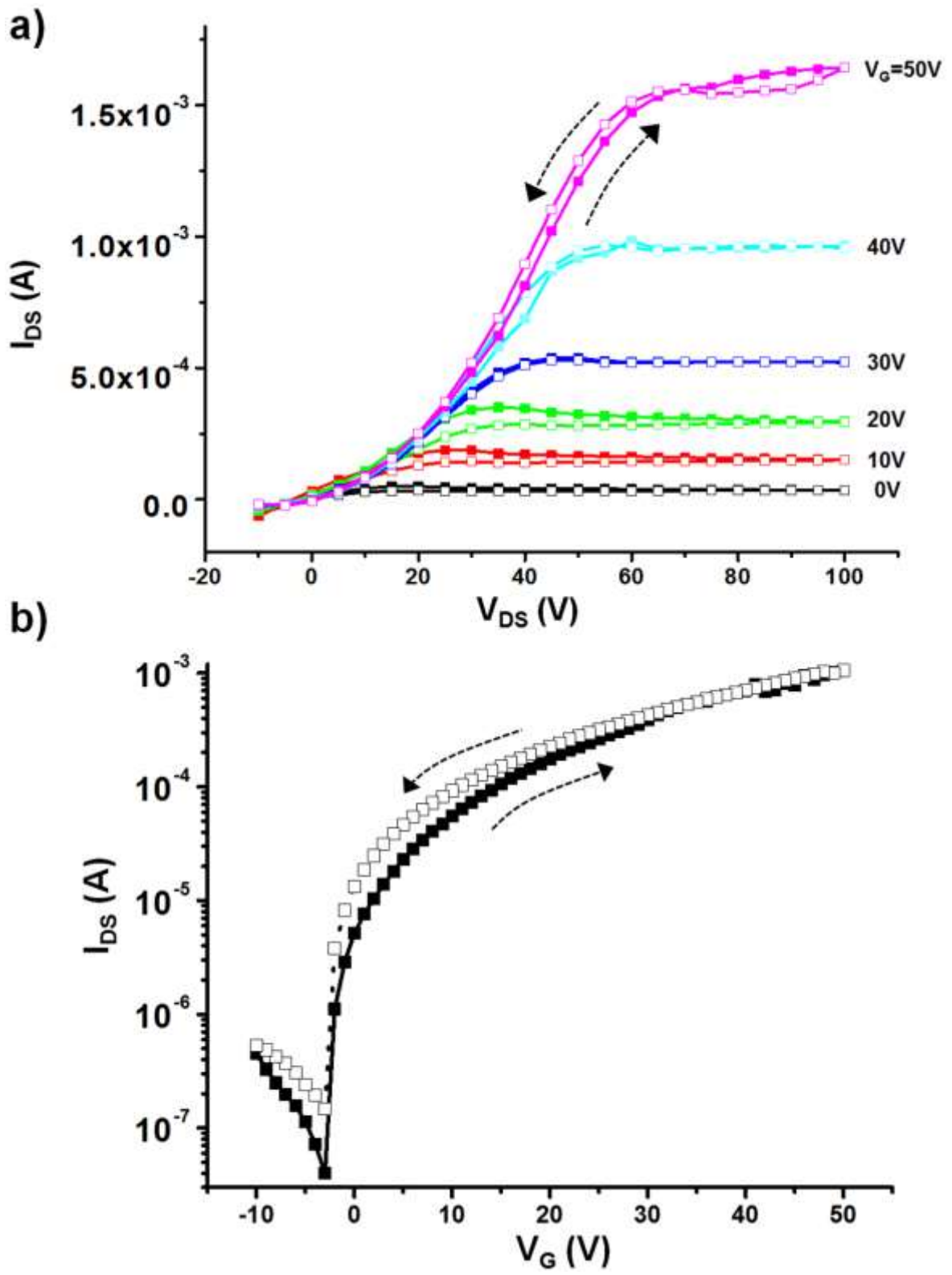


Fig 2

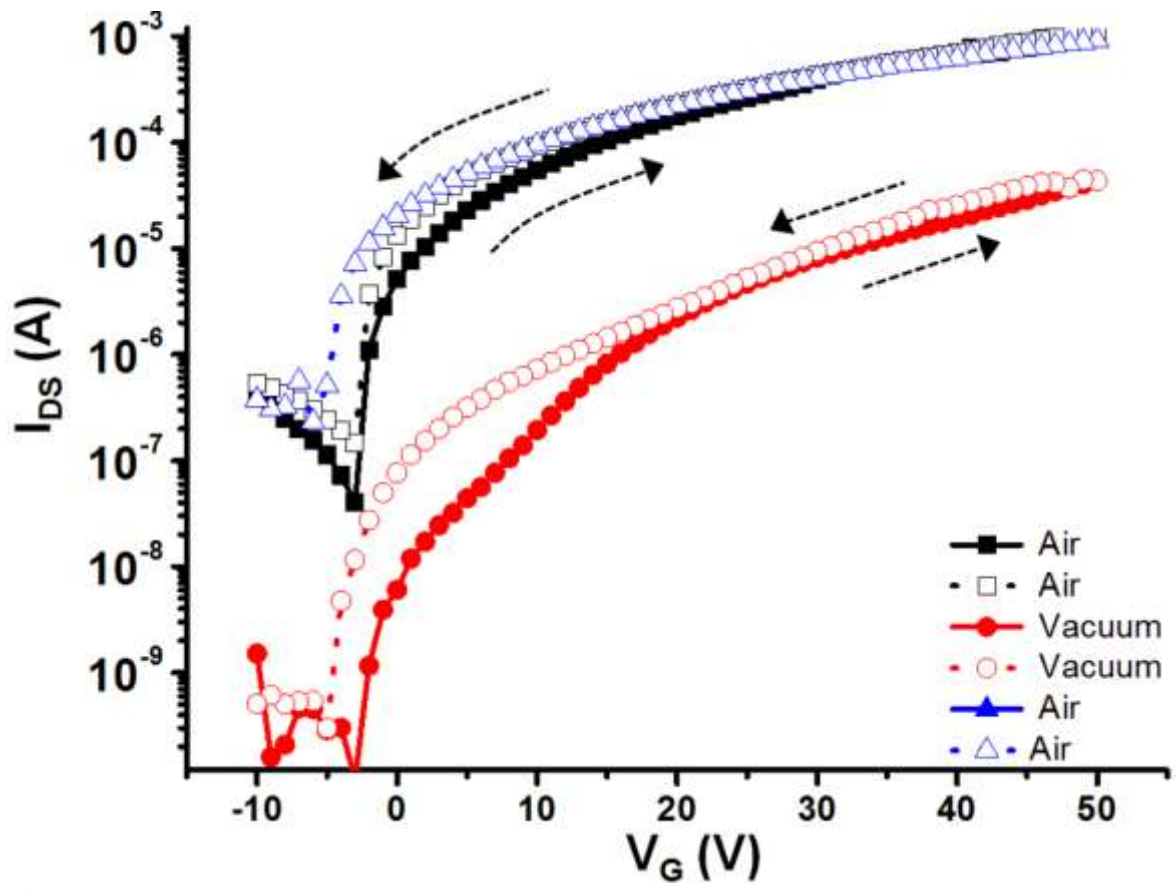


Fig 3

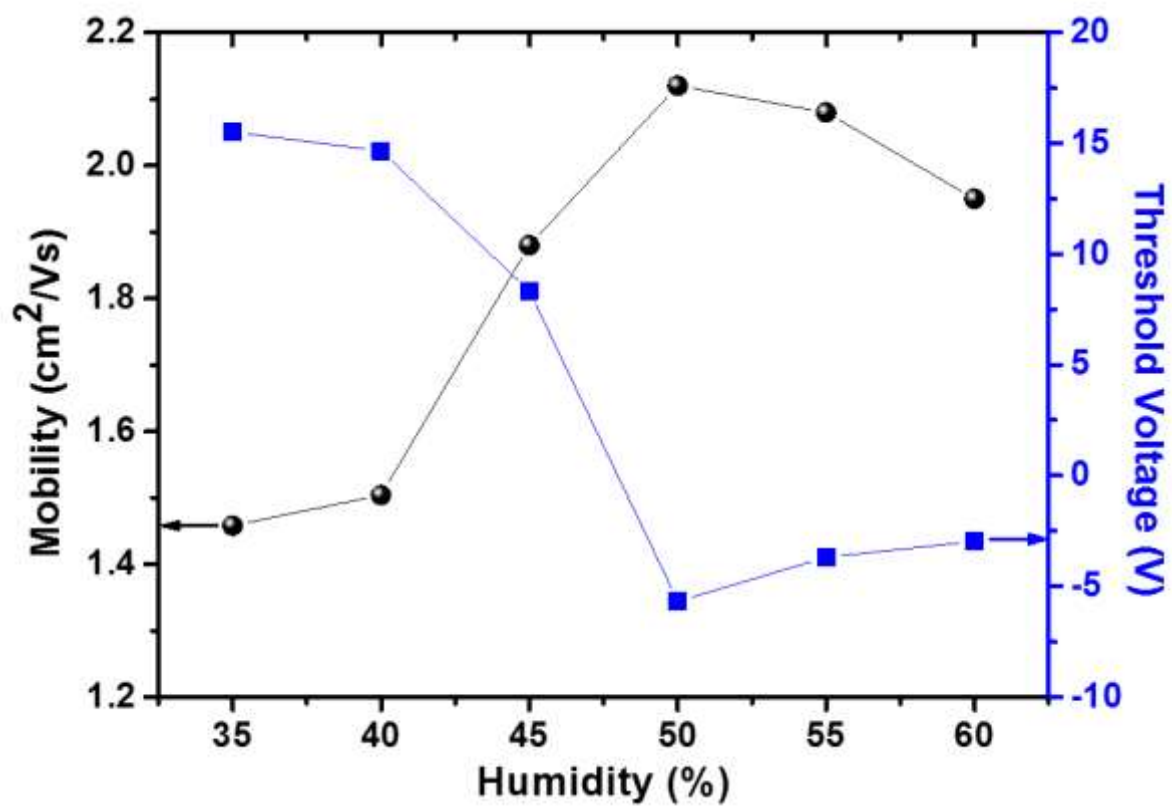


Fig 4